

Statistical analysis of aftershock sequences related with two major Nepal earthquakes: April 25, 2015, M_W 7.8, and May 12, 2015, M_W 7.2

Prasanta Chingtham¹, Babita Sharma^{1,*}, Sumer Chopra², Pareshnath SinghaRoy³

¹ National Centre for Seismology, Ministry of Earth Sciences, New Delhi, India

² Institute of Seismological Research, Gandhinagar, Gujarat, India

³ Indian Institute of Technology (Indian School of Mines), Dhanbad, India

Article history

Received April 5, 2016; accepted September 6, 2016.

Subject classification:

Nepal earthquakes; b -value; p -value; D_C .

ABSTRACT

Present study describes the statistical properties of aftershock sequences related with two major Nepal earthquakes (April 25, 2015, M_W 7.8, and May 12, 2015, M_W 7.2) and their correlations with the tectonics of Nepal Himalaya. The established empirical scaling laws such as the Gutenberg–Richter (GR) relation, the modified Omori law, and the fractal dimension for both the aftershock sequences of Nepal earthquakes have been investigated to assess the spatio-temporal characteristics of these sequences. For this purpose, the homogenized earthquake catalog in moment magnitude, M_W is compiled from International Seismological Center (ISC) and Global Centroid Moment Tensor (GCMT) databases during the period from April 25 to October 31, 2015. The magnitude of completeness, M_C , a and b -values of Gutenberg–Richter relationship for the first aftershock sequence are found to be 3.0, 4.74, 0.75 (± 0.03) respectively whereas the M_C , a and b -values of the same relationship for the second aftershock sequence are calculated to be 3.3, 5.46, 0.90 (± 0.04) respectively. The observed low b -values for both the sequences, as compared to the global mean of 1.0 indicate the presence of high differential stress accumulations within the fractured rock mass of Nepal Himalaya. The calculated p -values of 1.01 ± 0.05 and 0.95 ± 0.04 respectively for both the aftershock sequences also imply that the aftershock sequence of first main-shock exhibits relatively faster temporal decay pattern than the aftershock sequence of second main-shock. The fractal dimensions, D_C values of 1.84 ± 0.05 and 1.91 ± 0.05 respectively for both the aftershock sequences of Nepal earthquakes also reveal the clustering pattern of earthquakes and signifies that the aftershocks are scattered all around the two dimensional space of fractured fault systems of the Nepal region. The low b -value and low D_C observed in the temporal variations of b -value and D_C before the investigated earthquake (M_W 7.2) suggest the presence of high-stress concentrations in the thrusting regimes of the Nepal region before the failure of faults. Moreover, the decrease of b -value with the corresponding decrease of D_C observed in their temporal variations can primarily act as an indicator for possible prediction of major earthquakes in the study region.

1. Introduction

The physics of earthquakes can be easily understood with the help of aftershock sequences related with the main earthquakes [Kisslinger 1996]. The aftershocks are also associated with considerable amount of energy generated by the heterogeneous materials in the subsurface near the source and that may not be related to the main-shock [Hamdache et al. 2004]. The fundamental processes behind the occurrence of main-shock and aftershocks may be similar for relatively simple tectonics [Shcherbakov et al. 2006]. On the other hand, in a highly heterogeneous medium, the occurrence of earthquakes are demonstrated with respect to time and space by the combined effect of different tectonic processes [Rundle et al. 2003]. Therefore, the characteristics of the aftershock sequence of a particular main-shock are mostly controlled by tectonic settings, mode of fault failure and the properties of rocks in the affected area [Frohlich 1987, Kisslinger and Jones 1991]. The characteristics of the aftershock sequence always confer vital information from its spatial and temporal distributions [Kisslinger and Jones 1991]. The studies related to aftershock sequences are helpful in understanding the earthquake nucleation process and the heterogeneities of the Earth's crust near the asperity zones for seismic hazard mitigation in a region [Utsu 1961, Scholz 1968, Dieterich 1986].

Statistical analysis of an aftershock sequence can provide important and valuable information related to the physical mechanisms of earthquake occurrences [Utsu 1969]. However, statistical analysis of most of the aftershock sequences follows different kinds of well established scaling laws available in the statistical seis-

mology [Gross and Kisslinger 1994, Shcherbakov and Turcotte 2004, Narteau et al. 2005, Shcherbakov et al. 2005, Lolli and Gasperini 2006]. In the present study, three well known empirical scaling laws namely GR relation [Gutenberg and Richter 1954], the modified Omori law [Utsu 1961], and fractal correlation dimension [Grassberger and Procaccia 1983] are investigated for characterizing the aftershock generation processes. The GR law gives the frequency–magnitude characteristics of earthquakes [Gutenberg and Richter 1954] while the modified Omori law models the decay of an aftershock occurrence with respect to time [Utsu 1961]. Fractal dimension correlates with the strength of the clustering of aftershocks in a space [Grassberger and Procaccia 1983]. The statistical parameters obtained with these relationships can be used to describe the characteristics of an aftershock sequence [Shcherbakov et al. 2005]. Several researchers have examined the applicability of above mentioned empirical laws in various seismic regions across the world [Reasenber and Jones 1989, Reasenber and Jones 1994, Tsapanos 1995, Guo and Ogata 1997, Felzer et al. 2004, Schorlemmer et al. 2005, Shcherbakov et al. 2005, Nanjo et al. 2007]. The behavior of an aftershocks in a region may satisfy several scaling laws with a reasonably good agreement, even though the aftershock sequence exhibits different characteristics and may vary from place to place [Console and Catalli 2005].

In the present study, the statistical parameters of the aftershock sequences related to Nepal earthquakes (April 25, 2015, and May 12, 2015) have been examined. Also the dependency on the magnitude of the mainshock and its surrounding tectonic set-up has been established. For this purpose, both the aftershock sequences of Nepal are expressed in terms of the GR relation, the modified Omori law and the fractal dimension to evaluate the seismotectonics of the Nepal region. The temporal variations of b -value and D_c are also evaluated to examine the highly stressed pattern formed by the existence of seismic faults before the impending earthquakes in the Nepal region. Accordingly, the homogenized earthquake catalog having minimum magnitude, $M_w \geq 2.2$ has been compiled from International Seismological Center (ISC) during the particular period from April 25 to October 31, 2015. The present study is valuable and important in the sense that this provides statistical parameters which help in understanding the physics of recent earthquake sequence in Nepal Himalayan region. Finally, the estimated parameters from the above empirical scaling laws can be essentially useful for assessing the probabilistic seismic hazard, thereby integrating the role of aftershocks in the Nepal region.

2. Seismotectonics of the study area

Nepal Himalaya is positioned centrally along the great Himalayan mountains, formed during the collision between the Indian and Eurasian plates [Le Fort 1975, Bird 1978, Le Fort 1981]. This region has accumulated nearly 3 m of slip along with a converging rate of nearly 18 mm/yr along the Himalayan arc over the past 182 years [Ader et al. 2012]. The Main Central Thrust (MCT), the Main Boundary Thrust (MBT) and the Himalayan Frontal Thrust (HFT) are the major north dipping faults found in this region that have progressively migrated towards the south with experiencing repeated slips [Gansser 1964, DeCelles et al. 2001]. Presently, the most important feature here is the Main Himalayan Thrust (MHT), where the Indian lithospheric plate slides down the overriding Himalayan wedges [Schelling and Arita 1991, Zhao and Nelson 1993, Nelson et al. 1996]. Several researchers have carried out various studies and found the presence of a crustal ramp along the MHT, which is presently locked underneath the Lesser Himalaya [Bilham et al. 1997, Larson et al. 1999, Cattin and Avouac 2000, Bettinelli et al. 2006]. It has been observed that most of the earthquakes occur in this frictionally locked portion of the MHT in Nepal Himalaya [Pandey et al. 1995, 1999]. The continuous convergence of Indian and Eurasian plates results in the accumulation of strain energy beneath Himalaya, which is periodically released during large earthquakes [Mitra et al. 2015]. Many historical earthquakes have ruptured the locked segment of MHT [Lave et al. 2005, Kumar et al. 2006, Kumar et al. 2010] and this segment also has the potential to generate future large to great earthquakes [Khatti 1987, Bilham and Ambraseys 2005]. However, most of the small to moderate earthquakes have been observed in a narrow belt, called Himalayan seismic belt (HSB), which lies in between the MCT and the MBT [Ni and Barazangi 1984]. As such, the shortening rate of the India-Eurasia convergence is absorbed mainly by the MHT through coseismic, preseismic and post seismic slip [Bettinelli et al. 2006]. This absorption is generally supported by the evidences of crustal deformations that occurred on the MHT [Bettinelli et al. 2006, Ader et al. 2012].

Most recently, in between the rupture zone of 1505 and 1934 earthquakes, an earthquake named as Gorkha or Nepal earthquake of magnitude $M_w = 7.8$ occurred 77 km northwest of Nepal's capital Kathmandu on April 25, 2015. This earthquake ruptured a 55 km wide and shallow dipping ($\sim 7^\circ$) segment of the MHT, which tilted the Himalaya south-westward by nearly 5 m over the Indian plate [Denolle et al. 2015, Galetzka et al. 2015, Mitra et al. 2015]. It is also believed that the most damaging earthquake after the 1934 Bihar-Nepal

Correlation (X-Y)	Regression	Intercept α	Slope β	$\eta(\sigma_y^2/\sigma_x^2)$	Number of data points n
$M_S - M_W$	GOR	1.6603 (0.099)	0.7329 (0.017)	0.46	8
	OR	1.7137 (1.149)	0.7237 (0.197)	1	
	SR	1.8081	0.7072		
	ISR	-1.5293	0.7557		
$m_b - M_S$	GOR	-3.8228 (0.031)	1.9333 (0.007)	0.72	228
	OR	-3.5215 (0.234)	1.8568 (0.059)	1	
	SR	-0.7536	1.1538		
	ISR	4.8133	2.1849		
$M_L - M_S$	GOR	-9.3134 (0.068)	3.2956 (0.017)	0.72	275
	OR	-7.9512 (0.844)	2.9456 (0.216)	1	
	SR	-0.7536	1.1538		
	ISR	4.8133	2.1849		

Table 1. Values of the regression parameters (intercept α , slope β , ratio of error variances $\eta(\sigma_y^2/\sigma_x^2)$ and number of data points n) developed for the study region.

earthquake in the area, killing nearly 8500 people and destroying thousands of buildings and historical sites in and around the Kathmandu city of Nepal [Mitra et al. 2015, Parameswaran et al. 2015]. The toll and devastation was increased further by another major earthquake (M_W 7.2) which ruptured on May 12, 2015, in the eastern edge of the rupture area of main-shock [Mitra et al. 2015]. However, the energy dissipated from these two major earthquakes to the nearby faults may have also activated earthquakes in close proximity of the adjacent areas [Avouac et al. 2015, Bilham 2015]. These two earthquakes have generated lots of aftershocks to their east which make it important to study the behavior of the aftershock's patterns related to these earthquakes in this region for examining the futuristic seismicity pattern in the area.

3. Data and methodology

The data available in the ISC have been downloaded for carrying out the statistical analysis of the Nepal earthquake sequence during the time period from April 25 to October 31, 2015. Global Centroid Moment Tensor (GCMT) database have also been explored while converting different magnitude scales such as body-wave magnitude (m_b), surface wave magnitude (M_S) and local magnitude (M_L) present in the ISC data into a homogenized moment magnitude, M_W by adopting generalized orthogonal (distanced) regression techniques [Castellaro al. 2006, Lolli et al. 2014]. In this homogenization process, all the M_L and m_b entries reported in the catalog are initially converted into M_S by using the GOR technique established from the correla-

tions $M_L - M_S$ and $m_b - M_S$ (Table 1). Later, M_S entries along with the converted M_S entries are finally converted into M_W by using the regression relationships between M_S and M_W . Table 1 depicts the values of the regression parameters estimated from different regression techniques, i.e., generalized orthogonal (GOR), orthogonal (OR, with $\eta = 1$), standard least-squares (SR) and inverse standard-least squares (ISR) regressions developed in the study region. It is noteworthy to mention that a total of 790 earthquakes, including the two major earthquakes ($M_W \geq 7$), with minimum magnitude equal to M_W 2.2 have been documented in the homogenized catalog during this short span of time (Figure 1). The data comprises of 61 events ($\sim 8\%$) and 150 events ($\sim 19\%$) with magnitudes $M_W \geq 5.0$ and $M_W \geq 4.0$ respectively. The first major Nepal earthquake (M_W 7.8) that occurred on April 25, 2015, was epicentered at 28.28N and 84.79E. After that, 41 aftershocks with two strong events ($M_W \geq 6$) having almost the similar fault plane solution with the main-shock followed within 2 h of the main-shock [Mitra et al. 2015]. While the other major earthquake (M_W 7.2) which also have the same fault plane and source dynamics with main-shock of April 25, 2015, occurred at 27.77N and 86.17E on May 12 after 17 days (Table 2). This earthquake was followed by another aftershock event of M_W 6.3 and several aftershocks having magnitude $M_W \geq 5$ within the next 24 hour. Figure 1 depicts the epicenters of two major earthquakes and aftershock sequence for the particular period from April 25 to October 31, 2015. The earthquake parameters and the Centroid Moment Tensor (CMT) solutions for two major and three strong

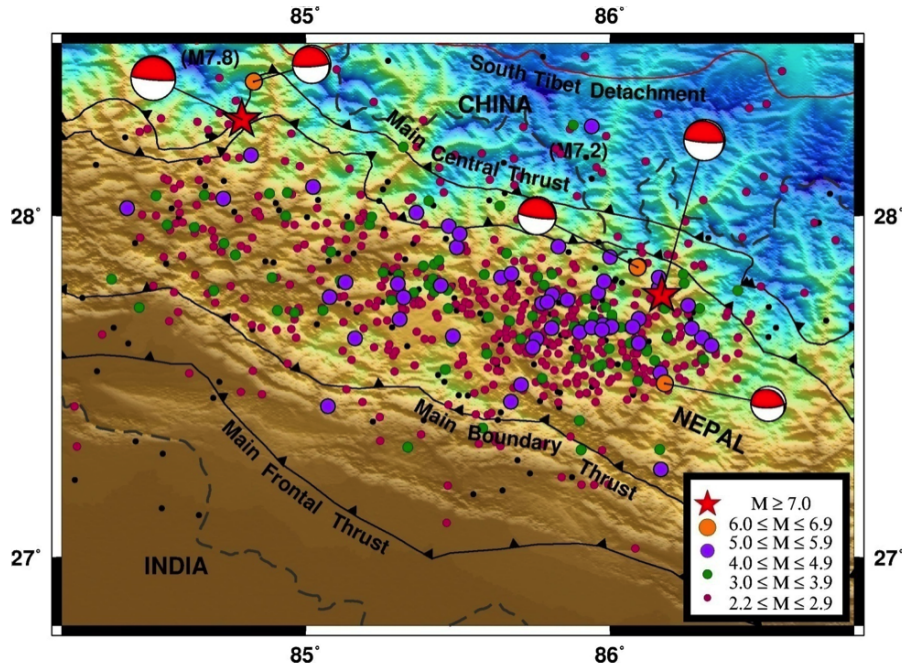


Figure 1. Tectonic map of Nepal and adjoining region drawn with the epicentral locations of aftershock sequences of Nepal earthquake during the period April 25 - October 31, 2015. Well determined focal mechanism solutions of the five largest earthquakes (listed in Table 2) are also shown with red color beach ball in the map. Stars show the epicenter of first (M_W 7.8) and second (M_W 7.2) main-shocks of Nepal earthquake sequence that occurred on April 25, 2015, and May 12, 2015, respectively.

Sl. No.	Date (yyyy.mm.dd)	Time (hh:mm:ss)	Latitude (N)	Longitude (E)	Depth (km)	Magnitude (M_W)	Focal mechanism solution		
							Strike	Dip	Rake
1	2015.04.25	06:11:26	28.28	84.79	12.0	7.8	293	7	108
2	2015.05.12	07:05:17	27.78	86.18	12.0	7.2	312	11	127
3	2015.04.26	07:09:10	27.85	86.09	17.4	6.8	296	10	108
4	2015.04.25	06:45:22	28.39	84.83	15.8	6.7	314	14	136
5	2015.05.12	07:36:51	27.51	86.19	20.1	6.2	303	23	123

Table 2. Details of the earthquake parameters and focal mechanism solutions of five largest earthquakes occurred in Nepal earthquake sequence. The information of the focal mechanism solutions are provided by the Global Centroid Moment Tensor (GCMT) database whereas the ISC catalog gives the other parameters of these earthquakes.

earthquakes in the sequence, reported by <http://www.isc.ac.uk/iscbulletin/seach> and <http://www.globalcmt.org/CMTsearch.html> are listed in Table 2.

Here, the maximum likelihood method is employed for fitting the statistical parameters of four different models of aftershock decay to the aftershock sequence of Nepal earthquake by using the observed data of the learning period (t_L) of 17 days [Ogata 1999, Woessner et al. 2004]. Following Woessner et al. [2004], the simple modified Omori model is finally applied to plot the forecasted curve of the aftershocks activity during the forecasted period (t_F) of 173 days. Goodness-of-fit is examined for the Akaike Information Criterion (AIC) model to the observed data by applying a Kolmogorov-Smirnov (KS) Test at a significance level of 0.05 as shown in Figure 2a. Even though, the AIC value (-3316.76) is very low, the KS statistic value (0.028571)

is found below the significant level. We have seen a strong inconsistency between the observed aftershock activity and the forecasted curve during the forecasted period (Figure 2a). This finally implies that the earthquake sequence in the period of study cannot be fitted by a simple modified Omori law, thereby violating the self-similar process of aftershock occurrences [Utsu 2002, Shcherbakov and Turcotte 2004]. However, the plot that obtained by subtracting the forecasted from the observed cumulative number of aftershocks during the period from May 12 to October 31, 2015, is found to finally fit well by a simple modified Omori law as depicted in Figure 2b. Moreover, the magnitude difference between the magnitude of the main-shock (M_W 7.8) and its largest aftershock (M_W 7.2) for this sequence is found to be 0.6 (i.e., $\Delta m = 0.6$). This implies that the sequence does not obey the Bath's law also [Bath 1965].

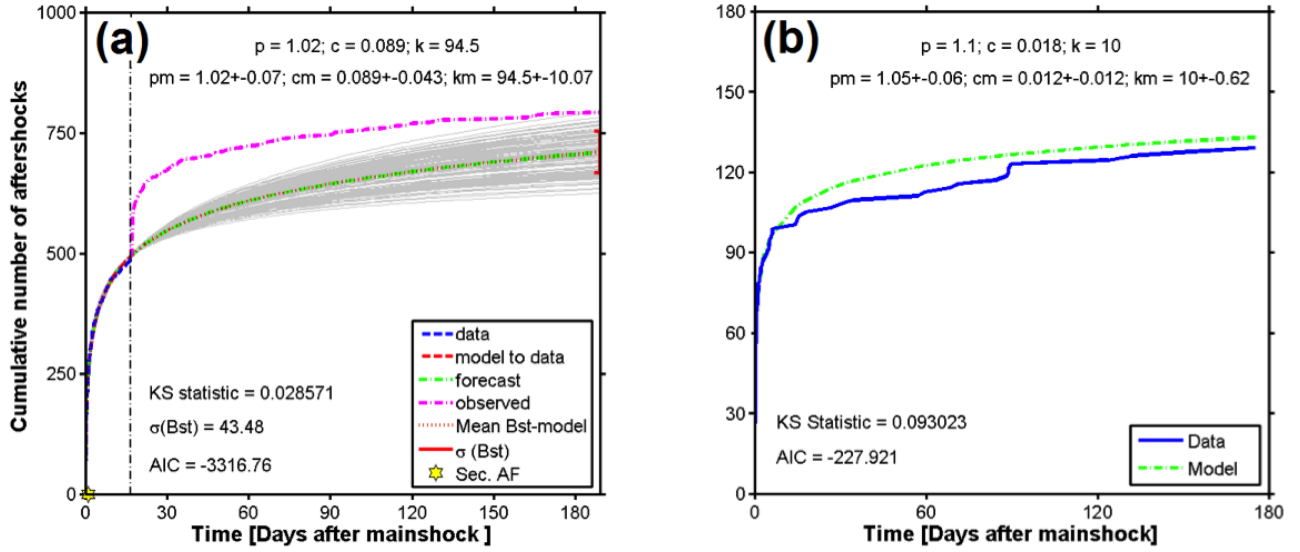


Figure 2. (a) The calculated model parameters and the forecast model of aftershocks activity for Nepal earthquake sequence based on observed data of 17 days learning period (t_L), estimated using maximum likelihood method. The bootstrap forecast models plotted as gray lines in the background fit with the modified Omori law. The brown line depicts the mean forecast model whereas the red bar shows the standard deviation of forecasted events at forecasted time (t_F). p , c and K indicates the modified Omori's parameters of the forecast model (green line) whereas pm , cm and km shows the modified Omori's parameters of the mean forecast model (brown line). The value of the standard deviation of the bootstrap model ($\sigma(Bst)$) is estimated to be 43.48. The vertical line indicates the end of the learning period. Star at time axis depicts the largest aftershock in learning period which is used to segregates the learning period in two time spans to fit the modified Omori's model parameters. (b) Observed cumulative number of aftershocks of the May 12 earthquake (a solid line) and the evaluated curve of the modified Omori formula fitted to the aftershock data during the period May 12 - October 31, 2015 (a broken line).

Alternatively, a slip model of M_W 7.2 [Avouac et al. 2015] event clearly indicates that the slip distribution of the May 12 earthquake falls outside the main-shock slip distribution. Depth section of M_W 7.2 event also falls on the ramp of the detachment plane which suggest that M_W 7.2 earthquake might be a triggered event [Avouac et al. 2015]. These evidences confirmed that the May 12 earthquake cannot be considered as an aftershock of the April 25 earthquake but can be regarded as a different earthquake, may be triggered by the main event. The statistical properties of both the aftershock sequences of the April 25 earthquake till before the occurrence of the May 12 earthquake have been studied carefully with respect to the GR frequency-magnitude statistics, the modified Omori law, and the fractal dimension, D_C , to assess the seismic characteristics of the Nepal region.

The frequency-magnitude distribution (FMD) of earthquakes is normally found to follow the GR [Gutenberg and Richter 1944]:

$$\log_{10} N(\geq m) = a - b.M \quad (1)$$

where $N(\geq M)$ gives the cumulative number of earthquakes defined in a specified space and time interval with magnitudes greater than or equal to M . Here, a -value indicates the seismic activity of a region and its value depends on many factors including maximum earthquake, background seismicity rate, area of study

and duration of catalog under observation [Chingtham et al. 2014]. However, b -value can be obtained from the slope of the frequency-magnitude distribution of earthquakes. The value lies in between 0.3 and 2, depending on the different tectonic conditions of the region [Utsu 1971, Udias 1999]. Hence, the crustal homogeneity with increasing stress regime can be associated with b -value lower than 1.0 whereas b -value more than 1.0 implies the region of crustal heterogeneity with low stress accumulation due to continued stress release [Wyss 1973, Wiemer and Wyss 2002, Thingbaijam et al. 2009, Yadav 2009, Yadav et al. 2012, Chingtham et al. 2014, Chingtham et al. 2015]. Moreover, higher magnitudes are also co-related with induced low b -value while lower magnitudes with high b -value [Nuannin et al. 2005]. The robust technique known as maximum likelihood is adopted to obtain the b -value [Aki 1965, Bender 1983, Utsu 1999] and is given by following relation:

$$b = \frac{\log_{10}(e)}{\log_{10}\left(m_{mean} - \left(m_t - \frac{\Delta m}{2}\right)\right)} \quad (2)$$

where m_{mean} and Δm are the mean magnitude and the size of magnitude bin respectively. The standard deviation, δb , of b -value can be estimated from the bootstrapping method [Chernick 1999, Schorlemmer et al. 2003]. This approach consists of computing b -value several times by random sampling with replacement of events in the catalog.

The temporal decay pattern of aftershocks is controlled by the modified Omori law [Utsu 1961, Utsu et al. 1995, Scholz 2002, Utsu 2002] which is given by the following equation:

$$N(t) = \frac{K}{(c+t)^p} \quad (3)$$

where $N(t)$ denotes the rate of occurrence of earthquakes at time t after the main-shock. K , c and p are the empirical constants. The complex post-seismic relaxation processes of a region can be unambiguously inferred from Equation (3) [Utsu 1961, Utsu et al. 1995]. The total number of events in a sequence defines the constant K , i.e., the aftershocks productivity while the parameter depicts the values related to unsuccessful identification of small aftershocks occurred in the beginning phase of the sequence [Kisslinger and Jones 1991, Utsu et al. 1995]. The slope estimated from the double-logarithmic plot between the occurrence rate of aftershocks and the time after the main-shock gives the most important parameter p -value which is the steepness of the aftershock's decay [Utsu 1961, Kisslinger and Jones 1991, Scholz 2002]. Although, the accepted global p -value is 1.0 for any aftershock sequence [Omori 1894] while it varies from 0.9 to 1.5, depending on several tectonic conditions such as geological heterogeneities and elastic strain buildup in the study region [Kisslinger and Jones 1991, Utsu et al. 1995].

The fractal dimension, D_C , of the earthquake depicts the strength of clustering of earthquakes through the power law exponent obtained from the number of pair of earthquake epicenters or focal depths measured

at different distance intervals [Kagan 2007]. D_C defines the fractured characteristics of the heterogeneous material by quantifying the relative strength of the spatial clustering of the events [Roy and Mondal 2009, 2012]. Hence, lower D_C value is associated with higher clustering of earthquakes while higher D_C value indicates uniform or random spatial distribution of events [Thingbaijam et al. 2008, Yadav et al. 2012, Chingtham et al. 2014]. Grassberger and Procaccia [1983] formulated the correlation integral method for estimating D_C and is given by

$$C(N, r) = \frac{2}{N(N-1)} \sum_{i=1}^N \sum_{j=i+1}^N H(r - |y_i - y_j|) \quad (4)$$

where $H(x)$ indicates the Heaviside step function whose value is 0 if $x < 0$, otherwise 1. N is the total number of earthquakes and y denotes the epicenters of the earthquakes. Finally, D_C value can be estimated from the slope of the plot between $\log_{10}(C(N, r))$ and $\log_{10}(r)$ [Narenberg and Essex 1990] obtained from the relation given below:

$$D_C = \lim_{r \rightarrow 0} \frac{\log_{10} C(N, r)}{\log_{10}(r)} \quad (5)$$

The variation of D_C , therefore, provides inclusive information on crustal heterogeneity and stability of the different tectonic zones in time and space [Turcotte 1986, Dimitriu et al. 1993]. Several researchers also imagined that it manifests the characterizing fractal patterns, thereby filling up the surrounding space qualitatively and quantitatively [Singh et al. 2012, Yadav et al. 2012, Bayrak et al. 2013]. So, clustering of earthquake

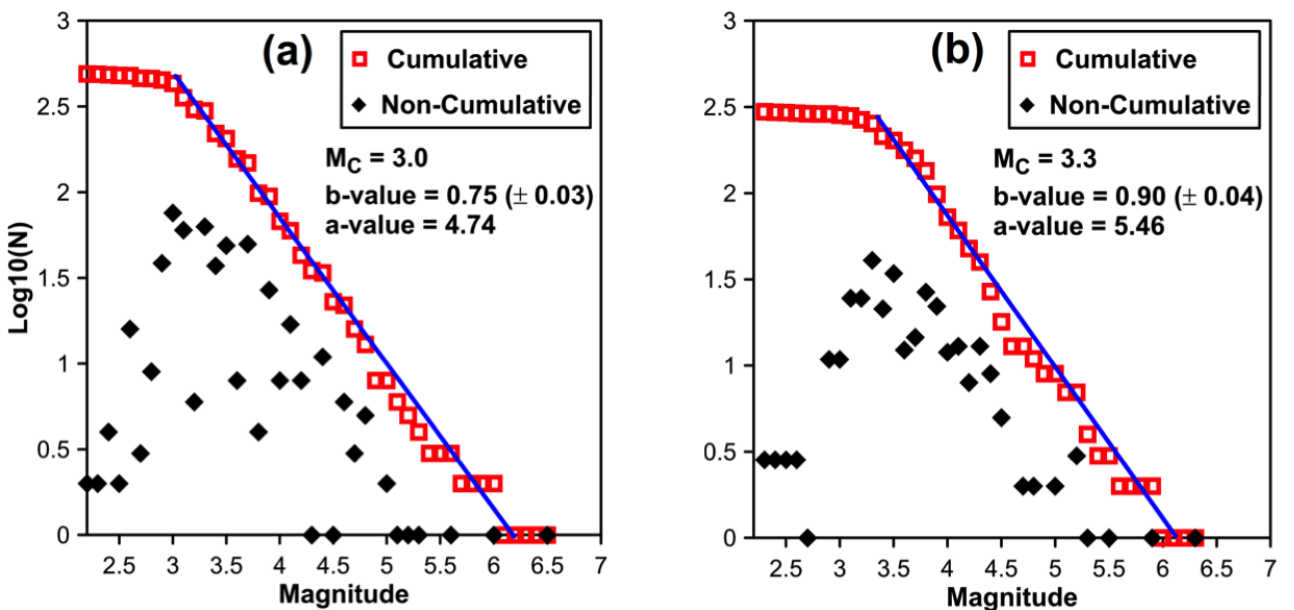


Figure 3. Frequency–magnitude distribution of GR relationship ($\log_{10}N = a - bM$) for both the aftershock sequences of (a) first (M_W 7.8) and (b) second (M_W 7.2) main-shocks of Nepal earthquake sequence.

epicenters into a point will induce D_C value close to zero while the value close to 1 suggests that the epicenters are distributed all along the line. Moreover, the D_C having values near to 2 and 3 signify that the epicenters are scattered all through the fractured surface and the crustal volume respectively [Khattri 1995, Singh et al. 2012, Bayrak et al. 2013].

The temporal variations of b -value and fractal dimension (D_C) have been accomplished by considering 100 events in each consecutive window with a slide of 10 events. In this sliding windowing technique, minimum 50 events with $M \geq M_C$ in each time window are essentially considered for determining the reliable b -value and D_C . The maximum likelihood method given by [Aki 1965, Bender 1983, Utsu 1999] is utilized for calculating b -value in each time window while D_C is estimated by employing correlation integral method given by Grassberger and Procaccia [1983] for the same time window. The reason behind the consideration of constant 100 events in each time window is to provide constant accuracy of b -value and D_C throughout the period of study. Moreover, it also primarily increases the statistical robustness on the estimated parameters for determining their potential as precursors in the highly tectonic regime of Nepal Himalaya [Nuannin 2006]. Later, the estimated values have been assigned to the mean of the corresponding time window. ZMAP software is employed for estimating the temporal variations of b -value [Wiemer 2001] whereas the temporal evolution of D_C is calculated by using FactalAnalyzer software developed by Roy and Gupta [2015].

4. Results and discussions

Mitra et al. [2015] suggested that the second major earthquake (M_W 7.2) is alleged to have occurred due to the propagation of stresses on the adjacent segment of the same fault of the first major earthquake (M_W 7.8). It is also accepted that the aftershock sequence of sec-

ond major earthquake may have been corrupted by the aftershock sequence of first major earthquake. The plot of aftershock's epicenters showed a large number of significant aftershocks have migrated from NNW to SSE direction, coinciding with the strike of one of the nodal plane (strike = 293, dip = 7, rake = 108) of the first major earthquake fault plane solution and is in accordance with the locked segment of MHT beneath the Nepal Himalayan region [Mitra et al. 2015]. This migration of aftershocks in the area shows that the rupture is propagated towards SE direction of the first major earthquake [Avouac et al. 2015].

The FMD plots for both the aftershock sequences of (M_W 7.8) and (M_W 7.2) main-shocks of Nepal earthquake sequence are presented by Figure 3a,b. The lowest magnitude level at which all the observed earthquakes that can be recorded in a particular space-time volume is defined by the completeness of magnitude, M_C and is computed by using maximum curvature method [Wiemer and Wyss 2000]. In this study, M_C is computed for both the aftershock sequences of first and second main-shocks of Nepal earthquake sequences and is equal to 3.0 and 3.3 respectively. By considering all the events above these completeness values, the a -value as well as the b -value with its standard deviation, b -value of GR relation for both the aftershock sequences are computed using maximum likelihood method given by Equation (2). The a and b -values for both the aftershock sequences are found to be 4.74 and 0.75 (± 0.03) respectively for first main-shock while for aftershock sequence related to second main-shock, the values are found to be 5.46 and 0.90 (± 0.04) respectively (Figure 3a,b, Table 3). The estimated b -values for both the sequences are lower than the global value of 1.0, which reveal that the main-shocks are considerably nucleated from a highly differential stressed regime [Wiemer and Katsumata 1999, Wiemer and Wyss 2002]. However, the observed low b -value for the aftershock sequence

Aftershock sequence	Gutenberg–Richter relation			Modified Omori law			Fractal dimension, D_C	Number of events
	M_C	a -value	b -value	c	K	p -value		
First main-shock (April 25, 2015, till before the occurrence of May 12, 2015, main-shock)	3.0	4.74	0.75 (± 0.03)	0.051 \pm 0.02	69.62 \pm 5.57	1.01 \pm 0.05	1.84 \pm 0.04	490
Second main-shock (May 12, 2015 - October 31, 2015)	3.3	5.46	0.90 (± 0.04)	0.01 \pm 0.008	19.06 \pm 1.95	0.95 \pm 0.04	1.91 \pm 0.07	298

Table 3. Summary of the results estimated from the established statistical parameters.

of first main-shock ($M_W 7.8$), as compared to the aftershock sequence of second main-shock ($M_W 7.2$) signifies that the aftershock sequence of first main-shock comprises of relatively larger magnitude aftershocks with scarcity of smaller size aftershocks. It is also notable that the maximum slips of nearly 4.5 m caused by both the April 25 and May 12 Nepal earthquakes produced large size asperities in the hypocentral areas of the MHT plane [Galetzka et al. 2015, Zhang et al. 2016], thereby generating larger size aftershocks which results in low b -values for both the aftershock sequences of Nepal earthquakes. Our results of low b -values in large asperity zones caused by large slips are found to be consistent with the findings of Irmak et al. [2012] for October 23, 2011, Turkey earthquake ($M_W = 7.1$).

The temporal decay rates of both the aftershock sequences of Nepal earthquakes are depicted by Figure 4a,b. The maximum likelihood method given by Equation (3) is employed to obtain the p , c and K -values in the modified Omori formula. The p -values 1.01 ± 0.05 and 0.95 ± 0.04 were estimated for both the aftershock sequences even though the maximum slip distributions for both the main-shocks are calculated to be around 4.5 m [Zhang et al. 2016]. The observed p -values are found to be near the global p -value of 1.0, which suggests that both the temporal decay patterns of the aftershock sequences can be effectively modeled by modified Omori law with p -value typically close to 1.0. But, the seismicity in the aftershock sequence of first main-shock decays relatively faster than the aftershock sequence of second main-shock (Figure 4 a,b). This also implies that the aftershock activities for the first main-shock have relatively shorter duration with respect to the aftershock activities for second main-shock [Bayrak

et al. 2013]. Moreover, a simple modified Omori law cannot be fitted to the high p -value region of aftershock sequence immediately after the April 25 earthquake because of the presence of large aftershocks at the early stage of its sequence. The associated c and K -values for the aftershock sequence of first main-shock ($M_W 7.8$) are estimated as 0.051 ± 0.02 and 69.62 ± 5.57 for 490 events between $0.005 \leq t \leq 17$ days while 0.01 ± 0.008 and 19.06 ± 1.95 are calculated by 298 events in the second aftershock sequence between $0.005 \leq t \leq 173$ days (Table 3). The incomplete removal of the background seismicity results in superposed sequences and subsequently provides large c -value for the first main-shock's aftershock sequence in comparison to second main-shock's aftershock sequence. In other words, the large c -value in collaboration with smaller magnitude incompleteness of the aftershock sequence of first main-shock reflects the more geometrically complex rupture propagation pattern of the April 25 earthquake's sequences relative to the May 12 earthquake's sequences as also observed by Yamakawa [1968] for the aftershock sequence of June 16, 1964, Niigata earthquake ($M_W 7.6$). From the final observations of b and p -values, we can here infer that the b -value of the FMD is predominantly controlled by stress heterogeneity and asperities while the maximum slip distribution during the main-shock and its aftershock activities governs the p -value distribution within the aftershock zone of Nepal earthquake.

The fractal dimensions, D_C , for both the aftershock sequences of first and second main-shocks of Nepal earthquakes are estimated from the log-log plot between the correlation integral formulated by Grassberger and Procaccia [1983] and distance between hypocenters as shown in Figure 5a,b. Table 3 displays

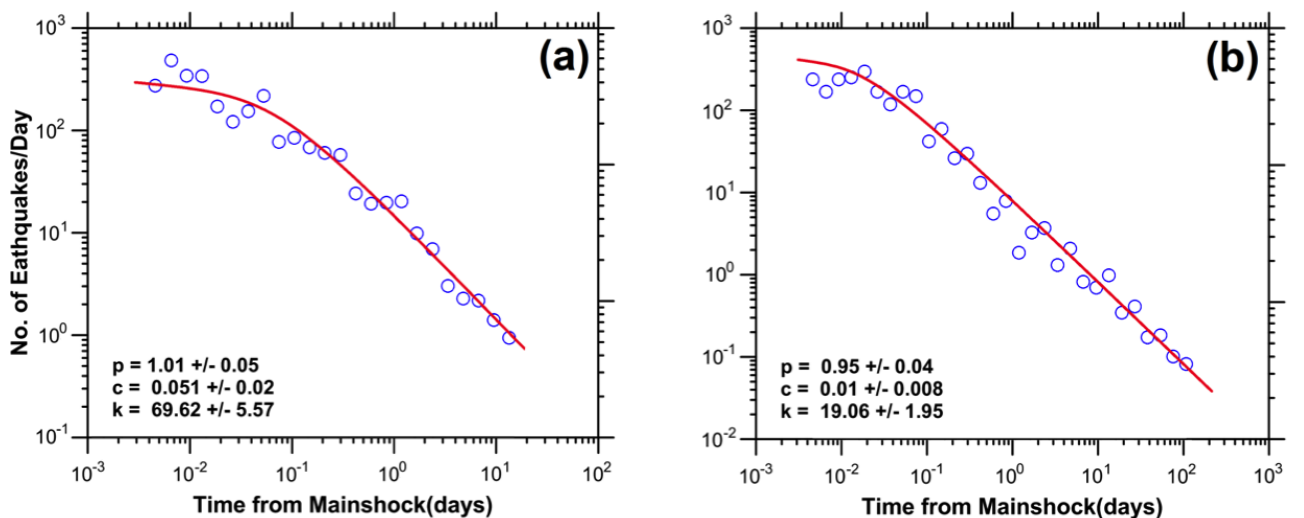


Figure 4. Temporal change of the number of aftershocks per day for both the aftershock sequences of (a) first ($M_W 7.8$) and (b) second ($M_W 7.2$) main-shocks of Nepal earthquake sequence along with their relevant respective parameters p , c and K -values in the modified Omori's Law.

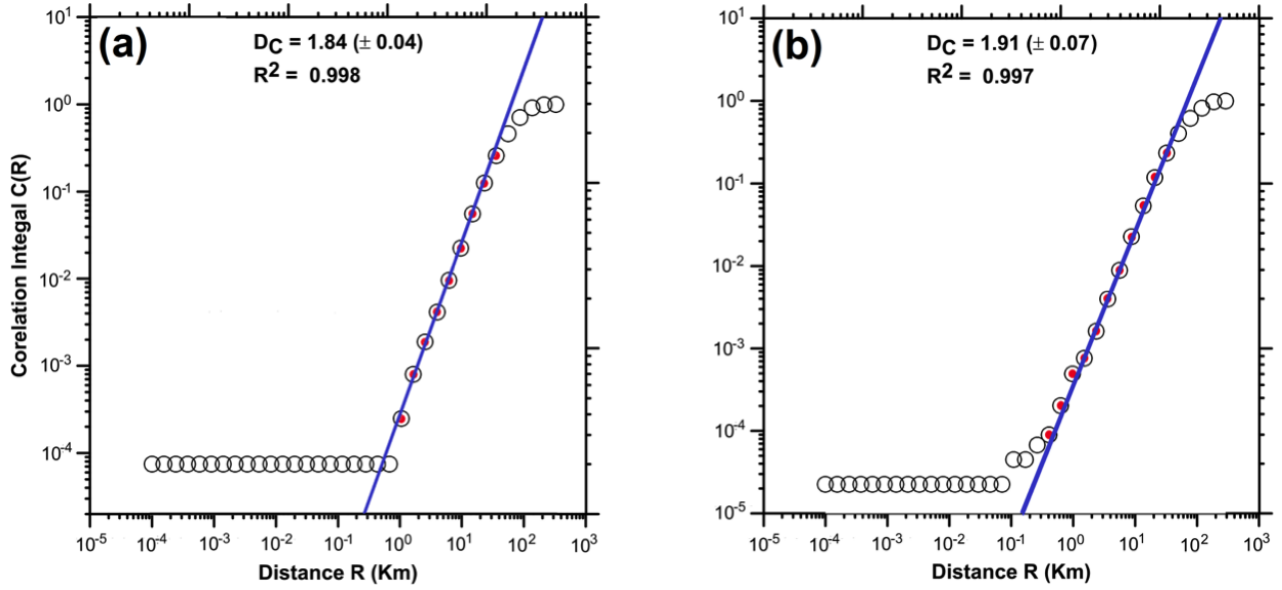


Figure 5. Plots of $\log C(r)$ against $\log r$ for determining the D_C of both the aftershock sequences of (a) first ($M_W 7.8$) and (b) second ($M_W 7.2$) main-shocks of Nepal earthquake sequence. R^2 corresponds to the correlation coefficient of the regression line.

that the calculated D_C for both the aftershock sequences are found to be 1.84 ± 0.04 for the first main-shock and 1.91 ± 0.07 for the second main-shock. The D_C close to 2 calculated for both the aftershock sequences of Nepal earthquake indicates that the epicentres of the aftershocks are scattered all around the two dimensional space. This also implies that the fractured fault networks of the Nepal region are randomly occupied by the distribution of aftershocks, thereby displaying the characteristics of two dimensions [Yadav et al. 2012]. Moreover, several researchers have done extensive studies on the relationship between the b -value of the GR law and the D_C of earthquakes [e.g., Hirata 1989, Turcotte 1992, Scholz 2002]. While considering that seis-

mic moment is proportional to the cube of the fault dimension, Aki [1981] suggested that the parameters are inter-related by $D_C = 3b/c$ where c gives the world average scaling constant (~ 1.5) between the logarithm of moment and magnitude of an earthquake [Kanamori and Anderson 1975]. For aftershock sequence of first main-shock, we have calculated $c = 1.22$ by assuming $D_C = 1.84$ and b -value = 0.75 while considering $D_C = 1.91$ and b -value = 0.90, we have found $c = 1.41$ for aftershock sequence of second main-shock of Nepal earthquake. These c -values are closer to the aforementioned statements and validate the relationship between b -value and D_C in the study region.

The temporal variation of b -value and its associ-

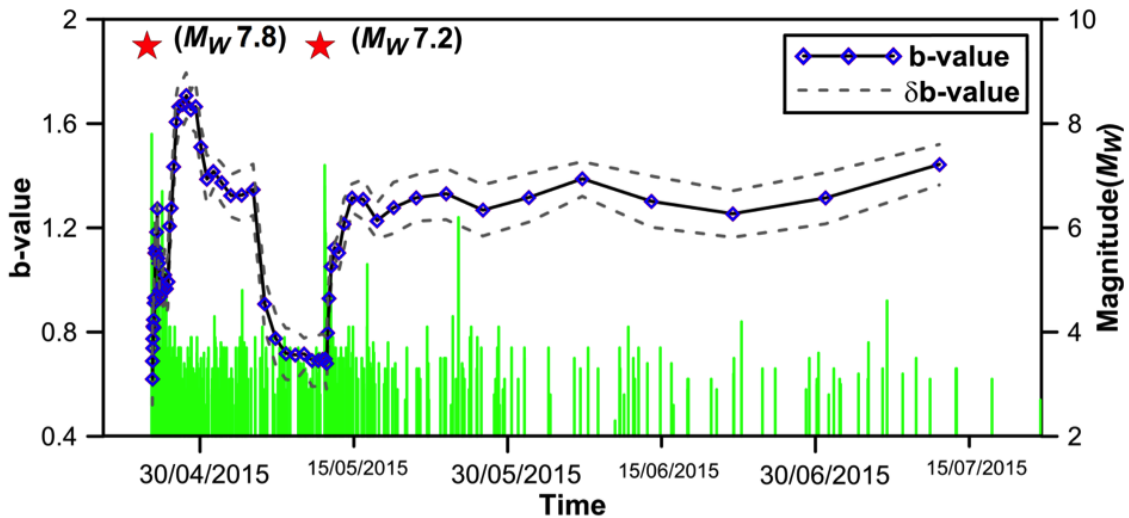


Figure 6. Temporal variation of b -value for the studied region. Dashed lines indicate the standard deviation and stars mark the times of occurrence of Nepal earthquakes for $M_W \geq 7$. Solid, vertical lines represent the time of occurrence and magnitude (right scale) of all recorded earthquakes. Date format: dd/mm/yyyy.

ated b -value are examined with respect to the occurrence of investigated earthquake (M_W 7.2, May 12, 2015) in the study region during the observational period from April 25 to October 31, 2015. The b -values are found varying in between 0.62 and 1.71 during the entire Nepal earthquake sequences as shown in Figure 6. However, the observed low b -values have been found decreasing from 1.35 to 0.69, starting from May 5 till the occurrence of May 12, 2015 (Table 4). This low b -value observed before the impending earthquake can be easily associated with the tectonic stress accumulation near the hypocentral region. These evidences of the relatively low b -value before the impending earthquake are in good agreement with the results presented by Wyss et al. [2000] and Wyss and Stefansson [2006]. Henderson et al. [1994] have also seen low b -value preceding large main-shocks while investigating the seismicity of the southern Californian region. Various studies have also confirmed that the temporal decrease in the b -value with relatively low seismicity rate before the large earthquakes may be considered as a forecasting indicator [Ogata and Katsura 1993, Wu et al. 2008, Papadopoulos et al. 2010]. In the present study, the b -values are observed to be increased significantly and found to remain in between 1.21 and 1.44 after the May 12, 2015, earthquake (Figure 6). These increased b -values significantly after a major earthquake can be considered as an evidence for stress reduction in and around the rupture areas.

Figure 7 depicts the significant temporal variation of D_C along with its standard deviation denoted by δD_C . Fluctuating nature of D_C with values varying between 0.67 and 1.72 can be seen from the temporal variation of D_C of Nepal earthquake sequence (Table 4). This

temporal variation of D_C have been found decreasing from 1.50 to 0.89, starting from May 6 till the occurrence of the May 12, 2015 earthquake, thereby exhibiting the similar trend with the temporal variation of b -value (Figures 6 and 7). It can be confirmed that the observed low D_C values before the impending earthquake (M_W 7.2) signifies high clustering near the epicentral area. This significant low D_C value along with highly clustered seismicity may indicate possible rupture nucleation point of the May 12 earthquake and can also be considered as an index for predicting future strong earthquake [Main 1992, Sammonds et al. 1992, Roy and Mondal 2010]. Similar to b -value variation, the decrease and then the increase D_C values observed in its temporal variation can be easily correlated with the clustering and scattering of earthquakes in a fractured material. In other words, the temporal variation of D_C reflects the stress accumulation and strain release pattern along the Himalaya region [Roy and Nath 2007]. The present analysis of D_C of seismicity further suggests the existence of complex stress pattern within the heterogeneous and fractured rock mass of the Nepal Himalayan region [Legrand et al. 1996, Oncel and Wilson 2004]. A positive correlation with low values has been observed between the temporal variations of b -value and D_C in the studied region as shown in Figures 6 and 7. This implies that the region exhibit high-stress concentrations with clustering of mainly large/major earthquakes as suggested by Oncel and Wyss [2000]. During this period of low b -value and low D_C , the region of the Earth's crust exhibit nearly "self-organized critical" (SOC) state such that the rupture propagation may eventually nucleate from this highly stressed region causing a strong earthquake [Roy and Mondal

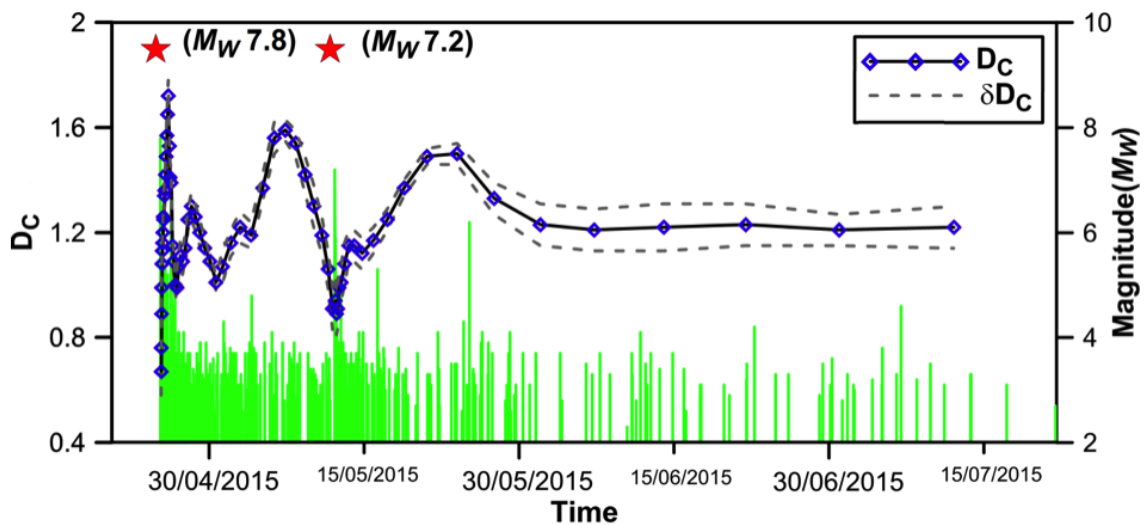


Figure 7. Temporal variation of D_C for the studied region. Dashed lines indicate the standard deviation and stars mark the times of occurrence of Nepal earthquake sequence for $M_W \geq 7$. Solid, vertical lines represent the time of occurrence and magnitude (right scale) of all recorded earthquakes. Date format: dd/mm/yyyy.

STATISTICAL ANALYSIS OF AFTERSHOCK SEQUENCES OF NEPAL EARTHQUAKES

Year	b -value	b -value	D_C	D_C	Year	b -value	b -value	D_C	D_C
2015.3132	0.62	0.10	0.67	0.09	2015.3297	1.42	0.07	1.07	0.06
2015.3133	0.69	0.10	0.76	0.01	2015.3318	1.37	0.08	1.16	0.05
2015.3133	0.74	0.10	0.89	0.09	2015.3344	1.32	0.08	1.22	0.06
2015.3134	0.77	0.10	0.99	0.09	2015.3372	1.32	0.10	1.19	0.05
2015.3134	0.82	0.10	1.08	0.06	2015.3404	1.35	0.10	1.37	0.05
2015.3135	0.85	0.10	1.13	0.06	2015.3435	0.91	0.10	1.56	0.06
2015.3136	0.82	0.10	1.16	0.06	2015.3464	0.77	0.10	1.59	0.04
2015.3137	0.91	0.10	1.2	0.06	2015.3492	0.72	0.10	1.54	0.05
2015.3138	0.93	0.10	1.26	0.05	2015.3518	0.71	0.10	1.42	0.07
2015.3139	1.10	0.10	1.25	0.04	2015.3541	0.72	0.06	1.3	0.08
2015.3140	1.12	0.10	1.34	0.05	2015.3563	0.69	0.10	1.19	0.07
2015.3142	1.10	0.06	1.36	0.05	2015.3579	0.69	0.10	1.06	0.07
2015.3143	1.18	0.01	1.42	0.05	2015.3591	0.69	0.10	0.91	0.08
2015.3145	1.27	0.02	1.49	0.06	2015.3598	0.70	0.09	0.94	0.09
2015.3147	1.08	0.02	1.57	0.07	2015.3602	0.68	0.10	0.89	0.08
2015.3149	1.06	0.00	1.65	0.06	2015.3605	0.80	0.10	0.91	0.08
2015.3151	0.96	0.01	1.72	0.06	2015.3608	0.93	0.07	0.99	0.08
2015.3154	0.94	0.04	1.53	0.07	2015.3614	1.05	0.07	1.01	0.07
2015.3156	0.98	0.01	1.41	0.06	2015.3623	1.12	0.02	1.08	0.08
2015.3159	0.96	0.02	1.39	0.05	2015.3635	1.10	0.07	1.15	0.06
2015.3162	0.97	0.09	1.15	0.03	2015.3649	1.21	0.09	1.15	0.06
2015.3166	1.02	0.10	1.09	0.04	2015.3670	1.31	0.05	1.12	0.06
2015.3170	0.97	0.10	1	0.03	2015.3700	1.31	0.08	1.17	0.05
2015.3174	0.99	0.10	0.99	0.05	2015.3738	1.23	0.07	1.25	0.04
2015.3179	1.21	0.10	1.07	0.05	2015.3782	1.28	0.10	1.37	0.03
2015.3183	1.27	0.10	1.11	0.06	2015.3844	1.31	0.09	1.49	0.03
2015.3189	1.43	0.10	1.09	0.05	2015.3924	1.33	0.10	1.5	0.04
2015.3196	1.61	0.10	1.14	0.05	2015.4023	1.27	0.10	1.33	0.06
2015.3204	1.66	0.10	1.25	0.04	2015.4148	1.32	0.09	1.23	0.08
2015.3213	1.67	0.09	1.3	0.05	2015.4292	1.39	0.07	1.21	0.08
2015.3223	1.71	0.09	1.26	0.05	2015.4478	1.30	0.10	1.22	0.09
2015.3235	1.65	0.07	1.2	0.05	2015.4697	1.25	0.09	1.23	0.08
2015.3248	1.66	0.10	1.14	0.04	2015.4947	1.31	0.10	1.21	0.06
2015.3263	1.51	0.08	1.09	0.02	2015.5254	1.44	0.08	1.22	0.08
2015.3279	1.39	0.09	1.01	0.03					

Table 4. Values for each consecutive 100 events time-windows of b -value and fractal dimension D_C , during the period April 25 - October 31, 2015.

2012]. Lu et al. [2005] also suggests that the decrease of D_C with the corresponding decrease of b -value can act as an index for possible prediction of earthquakes. However, the physical characteristics for this earth-

quake triggering based on the reduction of D_C or b -value have to be examined more carefully, especially at critical failure, for considering this index as a reliable predictor [Roy and Mondal 2012].

5. Conclusion

The statistical properties of the Nepal earthquake sequences have been investigated to assess the seismic characteristics of the study region. For this purpose, the statistical parameters such as b -value of GR relationship, p -value of aftershocks temporal decay and fractal dimension, D_C have been calculated and analysed for the aftershock sequences of first (M_W 7.8) and second (M_W 7.2) main-shocks of Nepal earthquake sequences, utilizing the homogenized earthquake catalog (M_W) compiled from ISC and GCMT during the period from April 25 to October 31, 2015. The Nepal earthquake sequence, thus, presents the complexity of present day tectonics in Nepal. The b -values, i.e., $0.75 (\pm 0.03)$ and $0.90 (\pm 0.04)$ for both the aftershock sequences that are found lower than the global mean value of 1.0, which implies the complexities in terms of heterogeneities present in the ruptured zones. The relatively low b -value of the first main-shock's aftershock sequence with respect to second main-shock's aftershock sequence suggests the presence of larger magnitude earthquakes in the sequence. This evidence is also supported by the occurrence of 41 aftershocks after the April 25, 2015, earthquake within 24 hours. The p -value obtained for the aftershock sequence of first main-shock (1.01 ± 0.05) shows relatively faster decay pattern with lesser stress dissipation time than the aftershock sequence of second main-shock (0.95 ± 0.04). The respective values of D_C for both the aftershock sequences of first (1.84 ± 0.04) and second (1.91 ± 0.07) main-shocks of Nepal earthquake sequences indicate that the aftershocks are randomly scattered all around the two dimensional planar surface being filled up by fractures in the Nepal Himalaya. Both the aftershock sequences of the Nepal earthquakes exhibit positive correlation between fractal dimension (D_C) and b -value, thereby following the classical Aki's formula ($D_C = 3b/1.5$). The temporal variations of b -value and D_C are also investigated to examine the increased stress accumulations in the heterogeneous crust and the clustering of events related to the preparation of earthquake processes in Nepal Himalayan region. Furthermore, the distinct drops of b -value (~ 0.60) caused by the increased tectonic stress accumulation in the study region can be easily associated with the occurrence of a major earthquake (M_W 7.2) on May 12, 2015. Similarly, the low D_C value observed before the impending earthquake of May 12, 2015 (M_W 7.2) also exhibits the rupture nucleation points of stressed region of Nepal Himalaya. However, the positive correlations between b -value and D_C can act as an indicator for possible prediction of earthquakes in a region. Statistical parameters estimated in the present study describe the tectonic behavior of the study area

which infers the high stress accumulation in the heterogeneous and fractured rock matrix of the Nepal Himalayan region. More and more data is required to get further robust results for finding the futuristic earthquake scenarios, which in turn for characterizing the seismic regime in a better way.

Acknowledgements. Authors sincerely thank Dr. Shailesh Nayak, Former Secretary and Distinguished Professor and Scientist, Ministry of Earth Sciences, for his consistent motivation. Dr. V.K. Gahlaut, Director, National Center of Seismology (NCS) is gratefully acknowledged for encouragement to accomplish this piece of research. Authors are also thankful to anonymous reviewers and Editors for their constructive comments that significantly improved the manuscript.

References

- Ader, T., J.P. Avouac, J. Liu-Zeng, H. Lyon-Caen, L. Bollinger, J. Galetzka, M. Thomas, K. Chanard, S.N. Sapkota, S. Rajaure, P. Shrestha, L. Ding and M. Flouzat (2012). Convergence rate across the Nepal Himalaya and interseismic, coupling on the main Himalaya thrust: Implications for seismic hazard, *J. Geophys. Res.*, 117, B04403; doi:10.1029/2011JB009071.
- Aki, K. (1965). Maximum likelihood estimate of b in the formula $\log N = a - b.M$ and its confidence limits, *B. Earthq. Res. I. Tokyo*, 43, 237-239.
- Aki, K. (1981). A probabilistic synthesis of precursory phenomena, In: D.W. Symposium and P.G. Richards (eds.), *Earthquake Prediction: An International Review*, AGU, Washington, D.C., 566-574.
- Avouac, J.P., L. Meng, S. Wei, W. Wang and J.P. Ampuero (2015). Lower edge of locked Main Himalayan Thrust unzipped by the 2015 Gorkha earthquake, *Nat. Geosci.*, 8, 708-711; doi:10.1038/ngeo2518.
- Bath, M. (1965). Lateral inhomogeneities of the upper mantle, *Tectonophysics*, 2, 483-514.
- Bayrak, Y., R.B.S. Yadav, D. Kalafat, T.M. Tsapanos, H. Çinar, A.P. Singh, E. Bayrak, Yilmaz, S., F. Öcal and G. Koravos (2013). Seismogenesis and earthquake triggering during the Van (Turkey) 2011 seismic sequence, *Tectonophysics*, 601, 163-176.
- Bender, B. (1983). Maximum-likelihood estimation of b -values for magnitude grouped data, *B. Seismol. Soc. Am.*, 73 (3), 831-851.
- Bettinelli, P., J.P. Avouac, M. Flouzat, F. Jouanne, L. Bollinger, P. Willis and G. Chitrakar (2006). Plate motion of India and Interseismic strain in the Nepal Himalaya from GPS and DORIS measurements, *J. Geod.*, 80, 567-589.
- Bilham, R., K. Larson and J. Freymuller (1997). GPS measurements of present-day convergence across the Nepal Himalaya, *Nature*, 386, 61-64.
- Bilham, R., and N. Ambraseys (2005). Apparent Hi-

- malayan slip deficit from the summation of seismic moments for Himalayan earthquakes, 1500-2000, *Curr. Sci. India*, 88, 1658-1663.
- Bilham, R. (2015). *Seismology: Raising Kathmandu*, *Nat. Geosci.*, 8, 582-584; doi:10.1038/ngeo2498.
- Bird, P. (1978). Initiation of intercontinental subduction in the Himalaya, *J. Geophys. Res.*, 83, 4975-4987.
- Castellaro, S., F. Mulargia and Y.Y. Kagan (2006). Regression problems for magnitudes, *Geophys. J. Int.*, 165, 913930.
- Cattin, R., and J. Avouac (2000). Modeling mountain building and the seismic cycle in the Himalaya of Nepal, *J. Geophys. Res.*, 105, 13389-13407.
- Chernick, M.R. (1999). *Bootstrap methods: a practitioner's guide*, Wiley series in probability and statistics, Wiley, New York.
- Chingtham, P., S. Chopra, I. Baskoutas and B.K. Bansal (2014). An assessment of seismicity parameters in northwest Himalaya and adjoining regions, *Nat. Hazards*, 71, 1599-1616; doi:10.1007/s11069-013-0967-5.
- Chingtham, P., R.B.S. Yadav, S. Chopra, A.K. Yadav, A.K. Gupta and P.N.S. Roy (2015). Time-dependent seismicity analysis in the Northwest Himalaya and its adjoining regions, *Nat. Hazards*, 1-18; doi:10.1007/s11069-015-2031-0.
- Console, R., and F. Catalli (2005). A physical model for aftershocks triggered by dislocation on a rectangular fault, Submitted to Special Issue Tectonophysics, EGU-NP3.06 Session Vienna; arXiv:physics/0505033 [physics.geo-ph].
- DeCelles, P.G., D.M. Robinson, J. Quade, T.P. Ojha, C.N. Garzzone, P. Copeland and B.N. Upreti (2001). Stratigraphy, structure, and tectonic evolution of the Himalayan fold-thrust belt in western Nepal, *Tectonics*, 20(4), 487-509.
- Denolle, M.A., W. Fan and P.M. Shearer (2015). Dynamics of the 2015 M7.8 Nepal earthquake, *Geophys. Res. Lett.*, 42, 7467-7475; doi:10.1002/2015GL065336.
- Dieterich, J.H. (1986). A model for the nucleation of earthquake slip, In: *Earthquake Source Mechanics*, Geophysical Monograph Series, vol. 37, edited by S. Das et al., AGU, Washington, D.C., 37-49.
- Dimitriu, P.P., E.E. Papadimitriou, B.C. Papazachos and T.M. Tsapanos (1993). Global study of the distribution of earthquakes in space and in time by the fractal method, In: *Proceedings of the 2nd International Conference Geophysical Union of Greece (Florina, Greece, May 5-8, 1993)*, 1, 164-174.
- Felzer, K.R., R.E. Abercrombie and G. Ekström (2004). A common origin for aftershocks, foreshocks, and multiplets, *B. Seismol. Soc. Am.*, 94 (1), 88-98; doi:10.1785/0120030069.
- Frohlich, C. (1987). Aftershocks and temporal clustering of deep earthquakes, *J. Geophys. Res.*, 92, 13944-13956.
- Galetzka, J., J.P. Avouac, J.F. Genrich and K.W. Hudnut (2015). Slip pulse and resonance of Kathmandu basin during the 2015 Mw 7.8 Gorkha earthquake, Nepal imaged with geodesy, *Science*, 06 Aug 2015; doi:10.1126/science.aac6383.
- Gansser, A. (1964). *Geology of the Himalayas*, Wiley-Interscience, New York.
- Grassberger, P., and I. Procaccia (1983). Characterization of strange attractors, *Phys. Rev. Lett.*, 50, 346-349.
- Gross, S.J., and C. Kisslinger (1994). Test of models of aftershock rate decay, *B. Seismol. Soc. Am.*, 84, 1571-1579.
- Guo, Z.Q., and Y. Ogata (1997). Statistical relations between the parameters of aftershocks in time, space, and magnitude, *J. Geophys. Res.*, 102 (B2), 2857-2873.
- Gutenberg, B., and C.F. Richter (1944). Frequency of earthquakes in California, *B. Seismol. Soc. Am.*, 34, 185-188.
- Gutenberg, B., and C.F. Richter (1954). *Seismicity of the Earth and Associated Phenomena*, Princeton Univ. Press, Princeton, N.J.
- Hamdache, M., J.A. Peláez and K. Yelles Chauche (2004). The Algiers, Algeria earthquake (M_W 6.8) of 21 May 2003: Preliminary report, *Seismol. Res. Lett.*, 75, 360-367.
- Henderson, J., I.G. Main, R.G. Pearce and M. Takeya (1994). Seismicity in north-eastern Brazil - fractal clustering and the evolution of the b -value, *Geophys. J. Int.*, 116, 217-226.
- Hirata, T. (1989). Fractal Dimension of Fault Systems in Japan: Fractal structure in rock fracture geometry at various scales, *Pure Appl. Geophys.*, 131, 157-170.
- Irmak, T.S., B. Doğan and A. Karakaş (2012). Source mechanism of the 23 October 2011 Van (Turkey) earthquake ($M_w = 7.1$) and aftershocks with its tectonic implications, *Earth Planets Space*; <http://dx.doi.org/10.5047/eps.2012.05.002>.
- Kagan, Y.Y. (2007). Earthquake spatial distribution: the correlation dimension, *Geophys. J. Int.*, 168, 1175-1194.
- Kanamori, H., and D.L. Anderson (1975). Theoretical basis of some empirical relations in seismology, *B. Seismol. Soc. Am.*, 65, 1073-1095.
- Khattari, K.N. (1987). Great earthquakes, seismicity gaps and potential for earthquake disaster along the Himalaya plate boundary, *Tectonophysics*, 138, 79-92.
- Khattari, K.N. (1995). Fractal description of seismicity of India and inferences regarding earthquake hazard, *Curr. Sci. India*, 69, 361-366.

- Kisslinger, C., and L.M. Jones (1991). Properties of aftershocks in southern California, *J. Geophys. Res.*, 96, 11947-11958.
- Kisslinger, C. (1996). Aftershocks and fault-zone properties, *Adv. Geophys.*, 38, 1-36; doi:10.1016/S0065-2687(08)60019-9.
- Kumar, S., S.G. Wesnousky, T.K. Rockwell, R.W. Briggs, V.C. Thakur and R. Jayangondaperumal (2006). Paleoseismic evidence of great surface rupture earthquakes along the Indian Himalaya, *J. Geophys. Res.*, 111 (B03304); doi:10.1029/2004JB003309.
- Kumar, S., S.G. Wesnousky, R. Jayangondaperumal, T. Nakata, Y. Kumahara and V. Singh, (2010). Paleoseismological evidence of surface faulting along the northeastern Himalayan front, India: Timing, size, and spatial extent of great earthquakes, *J. Geophys. Res.*, 115 (B12422); doi:10.1029/2009JB006789.
- Larson, K., R. Burgmann, R. Bilham and J.T. Freymueller (1999). Kinematics of the India-Eurasia collision zone from GPS measurements, *J. Geophys. Res.*, 104, 1077-1093.
- Lave, J., D. Yule, S. Sapkota, K. Basant, C. Madden, M. Attal and R. Pandey (2005). Evidence for a Great Medieval Earthquake (1100 A.D.) in the Central Himalayas, Nepal, *Science*, 307, 1302-1305.
- Le Fort, P. (1975). Himalaya: the collided range. Present knowledge of the continental arc, *Am. J. Sci.*, 275A, 1-44.
- Le Fort, P. (1981). Manaslu leucogranite: a collision signature of the Himalaya, a model for its genesis and emplacement, *J. Geophys. Res.*, 86, 10545-10568.
- Legrand, D., A. Cisternas and L. Dorbath (1996). Multifractal analysis of the 1992 Erzincan aftershock sequence, *Geophys. Res. Lett.*, 23, 933-936.
- Lolli, B., and P. Gasperini (2006). Comparing different models of aftershock rate decay: the role of catalog incompleteness in the first times after mainshock, *Tectonophysics*, 423, 4359; doi:10.1016/j.tecto.2006.03.025.
- Lolli, B., P. Gasperini and G. Vannucci (2014). Empirical conversion between teleseismic magnitudes (m_b and M_s) and moment magnitude (M_w) at the Global, Euro-Mediterranean and Italian scale, *Geophys. J. Int.*, 199, 805-828; doi:10.1093/gji/ggu264.
- Lu, C., Y.W. Mai and H. Xie (2005). A sudden drop of fractal dimension: A likely precursor of catastrophic failure in disordered media, *Phil. Mag. Lett.*, 85 (1), 33-40.
- Main, I.G. (1992). Damage mechanics with long-range interactions – correlation between the seismic b -value and the fractal 2-point correlation dimension, *Geophys. J. Int.*, 111, 531-541.
- Mitra, S., P. Himangshu, K. Ajay, K. S. Shashwat, D. Sidharth and P. Debarchan (2015). The 25 April 2015 Nepal earthquake and its aftershocks, *Curr. Sci. India*, 108 (10), 1938-1943.
- Nanjo, K.Z., B. Enescu, R. Shcherbakov, D.L. Turcotte, T. Iwata and Y. Ogata (2007). Decay of aftershock activity for Japanese earthquakes, *J. Geophys. Res.*, 112, B08309; doi:10.1029/2006JB004754.
- Narenberg, M.A.A., and C. Essex (1990). Correlation dimension and systematic geometric effects, *Phys. Rev. A*, 42, 7065-7074.
- Narteau, C., P. Shebalin and M. Holschneider (2005). Onset of power law aftershock decay rates in southern California, *Geophys. Res. Lett.*, 32, L22312; doi:10.1029/2005GL023951.
- Nelson, K.D., W. Zhao, L.D. Brown, J. Kuo, J. Che, X. Liu, S.L. Klemperer, Y. Makovsky, R. Meissner, J. Mechie, R. Kind, F. Wenzel, J. Ni, J. Nabelek, L. Chen, H. Tan, W. Wei, A.G. Jones, J. Booker, M. Unsworth, W.S.F. Kidd, M. Hauck, D. Alsdorf, A. Ross, M. Cogan, C. Wu, E. Sandvol and M. Edwards (1996). Partially molten middle crust beneath southern Tibet: synthesis of project INDEPTH results, *Science*, 274 (5293), 1684-1688.
- Ni, J., and M. Barazangi (1984). Seismotectonics of the Himalayan collision zone: geometry of the underthrusting Indian plate beneath the Himalaya, *J. Geophys. Res.*, 80, 1142-1163.
- Nuannin, P., O. Kulhánek and L. Persson (2005). Spatial and temporal b -value anomalies preceding the devastating off coast of NW Sumatra earthquake of December 26, 2004, *Geophys. Res. Lett.*, 32, L11307; doi:10.1029/2005GL022679.
- Nuannin P. (2006). The Potential of b -value Variations as Earthquake Precursors for Small and Large Events, Digital Comprehensive Summaries of Uppsala Dissertations from the Faculty of Science and Technology, 183.
- Ogata, Y., and K. Katsura (1993). Analysis of temporal and spatial heterogeneity of magnitude frequency distribution inferred from earthquake catalogues, *Geophys. J. Int.*, 113, 727-738.
- Ogata, Y. (1999). Seismicity analysis through point-process modeling: a review, *Pure Appl. Geophys.*, 155, 471-507.
- Omori, F. (1894). On the aftershocks of earthquakes, *J. Coll. Imp. Univ. Tokyo*, 7, 111 (with Plates IV-XIX).
- Oncel, A.O., and M. Wyss (2000). Mapping the major asperities by minima of local recurrence time before the 1999 M 7.4 Izmit earthquake, In: *The Izmit and Duzce Earthquakes: Preliminary results*, Istanbul Technical University, Istanbul, 1-14.
- Oncel, A.O., and T. Wilson (2004). Correlation of seismotectonic variables and GPS strain measurements

- in western Turkey, *J. Geophys. Res.*, 109, B11306.
- Pandey, M., R. Tankudar, J.P. Avouac, J. Lave and J.P. Massot (1995). Interseismic strain accumulation on the Himalayan crustal ramp (Nepal), *Geophys. Res. Lett.*, 22, 751-754.
- Pandey, M., R. Tankudar, J.P. Avouac, J. Vergne and T. Heritier (1999). Seismotectonics of the Nepal Himalaya from a local seismic network, *J. Asian Earth Sci.*, 17, 703-712.
- Papadopoulos, G.A., M. Charalampakis, A. Fokaefs and G. Minadakis (2010). Strong foreshock signal preceding the L'Aquila (Italy) earthquake (M_w 6.3) of 6 April 2009, *Nat. Hazards Earth Sys.*, 10, 19-24; doi:10.5194/nhess-10-19-2010.
- Parameswaran, R.M., T. Natarajan, K. Rajendran, C.P. Rajendran, M. Rishav, M. Wood and H.C. Lekhak (2015). Seismotectonics of the April-May 2015 Nepal earthquakes: An assessment based on the aftershock patterns, surface effects and deformational characteristics, *J. Asian Earth Sci.*, 111, 161-174; doi:10.1016/j.jseaes.2015.07.030.
- Reasenber, P.A., and L.M. Jones (1989). Earthquake hazard after a main-shock in California, *Science*, 243, 1173-1176.
- Reasenber, P.A., and L.M. Jones (1994). Earthquake aftershocks – Update, *Science*, 265, 1251-1252.
- Roy, P.N.S., and A. Padhi (2007). Multifractal analysis of earthquakes in the southeastern Iran-Bam region, *Pure Appl. Geophys.*, 167, 2271-2290.
- Roy, P.N.S., and S.K. Mondal (2009). Fractal nature of earthquake occurrence in northwest Himalayan region, *J. Ind. Geophys. Union*, 13 (2), 63-68.
- Roy, P.N.S., and S.K. Mondal (2010). Identification of seismicity pattern for some destructive earthquakes, In: *Proceedings of the AGU Chapman Conference on Complexity and Extreme Events in Geosciences*, National Geophysical Research Institute, Hyderabad, India, 57.
- Roy, P.N.S., and S.K. Mondal (2012). Multifractal analysis of earthquakes in Kumaun Himalaya and its surrounding region, *J. Earth Syst. Sci.*, 121 (4), 1033-1047.
- Roy, P.N.S., and D.K. Gupta (2015). FractalAnalyzer: A matlab application for multifractal seismicity analysis, *Seismol. Res. Lett.*, 86 (5), 1424-1431.
- Rundle, J.B., D.L. Turcotte, R. Shcherbakov, W. Klein and C. Sammis (2003). Statistical physics approach to understanding the multiscale dynamics of earthquake fault systems, *Rev. Geophys.*, 41, 1019; doi:10.1029/2003RG000135.
- Sammonds, P.R., P.G. Meredith and I.G. Main (1992). Role of pore fluids in the generation of seismic precursors to shear fracture, *Nature*, 359, 228-230.
- Schelling, D., and K. Arita (1991). Thrust tectonics, crustal shortening and the structure of the Far Eastern Nepal Himalaya, *Tectonics*, 10, 851-862.
- Scholz, C.H. (1968). The frequency–magnitude relation of micro-fracturing in rock and its relation to earthquakes, *B. Seismol. Soc. Am.*, 58, 399-415.
- Scholz, C.H. (2002). *The Mechanics of Earthquakes and Faulting*, 2nd ed. Cambridge University Press, Cambridge.
- Schorlemmer, D., G. Neri, S. Wiemer and A. Mostaccio (2003). Stability and significance tests for *b*-value anomalies: example from the Tyrrhenian Sea, *Geophys. Res. Lett.*, 30, 1835; doi:10.1029/2003GL017335.
- Schorlemmer, D., S. Wiemer and M. Wyss (2005). Variations in earthquake-size distribution across different stress regimes, *Nature*, 437 (22), 539-542.
- Shcherbakov, R., and D.L. Turcotte (2004). A modified form of Båth's law, *B. Seismol. Soc. Am.*, 94 (5), 1968-1975; doi:10.1785/012003162.
- Shcherbakov, R., D.L. Turcotte and J.B. Rundle (2005). Aftershock statistics, *Pure Appl. Geophys.*, 162 (6-7), 1051-1076; doi:10.1007/s00024-004-2661-8.
- Shcherbakov, R., D.L. Turcotte and J.B. Rundle (2006). Scaling properties of the Parkfield aftershock sequence, *B. Seismol. Soc. Am.*, 96 (4B), S376-S384; doi:10.1785/0120050815.
- Singh, A.P., O.P. Mishra, R.B.S. Yadav and D. Kumar (2012). A new insight into crustal heterogeneity beneath the 2001 Bhuj earthquake region of Northwest India and its implications for rupture initiations, *J. Asian Earth Sci.*, 48, 31-42.
- Thingbaijam, K.K.S., S.K. Nath and A. Yadav (2008). Recent seismicity in northeast India and its adjoining region, *J. Seismol.*, 12, 107-123.
- Thingbaijam, K.K.S, P. Chingtham and S.K. Nath (2009). Seismicity in the north-west frontier province at the Indian–Eurasian plate convergence, *Seismol. Res. Lett.*, 80 (4), 599-608.
- Tsapanos, T.M. (1995). The temporal distribution of aftershock sequences in the subduction zones of the Pacific, *Geophys. J. Int.*, 123, 633-636.
- Turcotte, D.L. (1986). A fractal model for crustal deformation, *Tectonophysics*, 132, 261- 269.
- Turcotte, D.L. (1992). *Fractals and Chaos in Geology and Geophysics*, Cambridge University Press, New York, 221.
- Udias, A. (1999). *Principles of Seismology*, Cambridge University Press, New York.
- Utsu, T. (1961). A Statistical Study on the Occurrence of Aftershocks, *Geophys. Mag.*, 30, 521-605.
- Utsu, T. (1969). Aftershocks and earthquake statistics (I) - Some parameters which characterize an aftershock sequence and their interrelation, *J. Fac. Sci. Hokkaido Univ., Ser. VII*, 2, 129-195.

- Utsu, T. (1971). Aftershock and earthquake statistic (III): Analyses of the distribution of earthquakes in magnitude, time and space with special consideration to clustering characteristics of earthquake occurrence (1), *J. Faculty Sci. Hokkaido Univ., Ser. VII*, 3, 379-441.
- Utsu, T., Y. Ogata and R.S. Matsuura (1995). The centenary of the Omori formula for a decay law of aftershock activity, *J. Phys. Earth*, 43, 1-33.
- Utsu, T. (1999). Representation and analysis of the earthquake size distribution: a historical review and some new approaches, *Pure Appl. Geophys.*, 155, 509-535.
- Utsu, T. (2002). Statistical features of seismicity, In: W.H.K. Lee et al. (eds.), *International Handbook of Earthquake and Engineering Seismology Part A*, Academic Press, 719-732.
- Wiemer, S., and K. Katsumata (1999). Spatial variability of seismicity parameters in aftershock zones, *J. Geophys. Res.*, 104, 13135-13151.
- Wiemer, S., and M. Wyss (2000). Minimum magnitude of completeness in earthquake catalogues: Examples from Alaska, the western United States, and Japan, *B. Seismol. Soc. Am.*, 90, 859-869.
- Wiemer, S. (2001). A software package to analyze seismicity: ZMAP, *Seismol. Res. Lett.*, 72, 373-382.
- Wiemer, S., and M. Wyss (2002). Mapping spatial variability of the frequency-magnitude distribution of earthquakes, *Adv. Geophys.*, 45, 259-302.
- Woessner, J., E. Hauksson, S. Wiemer and S. Neukomm (2004). The 1997 Kagoshima (Japan) earthquake doublet: a quantitative analysis of aftershock rate changes, *Geophys. Res. Lett.*, 31, L03605; doi:10.1029/2003GL018858.
- Wu, Y.M., C.C. Chen, L. Zhao and C.H. Chang (2008). Seismicity characteristics before the 2003 Chengkung, Taiwan, earthquake, *Tectonophysics*, 457, 177-182.
- Wyss, M. (1973). Towards a physical understanding of the earthquake frequency distribution, *Geophys. J. Roy. Astr. S.*, 31, 341-359.
- Wyss, M., D. Schorlemmer and S. Wiemer (2000). Mapping asperities by minima of local recurrence time: The San Jacinto-Elsinore fault zones, *J. Geophys. Res.*, 105, 7829-7844.
- Wyss, M., and R. Stefansson (2006). Nucleation points of recent main-shocks in Southern Iceland, mapped by *b*-values, *B. Seismol. Soc. Am.*, 96, 599-608.
- Yadav, R.B.S. (2009). *Seismotectonic Modeling of NW Himalaya: A Perspective on Future Seismic Hazard*, PhD Thesis, Department of Earthquake Engineering, IIT Roorkee, India, 198 p.
- Yadav, R.B.S, Y. Bayrak, J.N. Tripathi, S. Chopra, A.P. Singh and E. Bayrak (2012). A probabilistic assessment of earthquake hazard parameters in NW Himalaya and the adjoining regions, *Pure Appl. Geophys.*; doi:10.1007/s00024-011-0434-8.
- Yamakawa, N. (1968). Foreshocks, aftershocks and earthquake swarms, (IV) Frequency decrease of aftershock activity in its initial and later stages, *Pap. Met. Geophys.*, 19, 109-119.
- Zhang, H., S. van der Lee and Z. Ge (2016). Multiarray rupture imaging of the devastating 2015 Gorkha, Nepal, earthquake sequence, *Geophys. Res. Lett.*, 43 (2), 584-491; doi:10.1002/2015GL066657.
- Zhao, W. J., and K.D. Nelson (1993). Deep seismic-reflection evidence for continental underthrusting beneath Southern Tibet, *Nature*, 366 (6455), 557-559.

*Corresponding author: Babita Sharma,
National Centre for Seismology, Ministry of Earth Sciences,
New Delhi, India; email: babita_s@rediffmail.com.